Engineering chiral induction in centrally functionalized *ortho*-phenylenes

Sumalatha Peddi[1], Juliana M. Livieri[1], Gopi Nath Vemuri[1], and C. Scott Hartley[1,*]

[1]Department of Chemistry & Biochemistry, Miami University, Oxford, Ohio 45056, United States

[*]scott.hartley@miamioh.edu

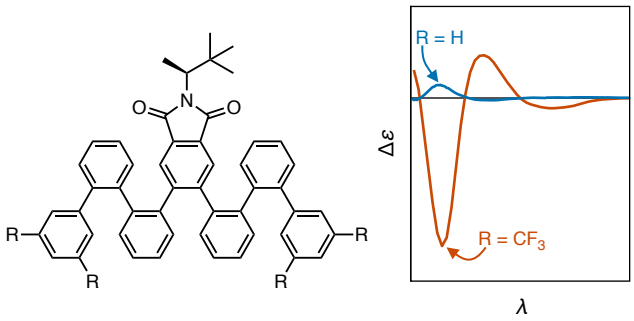

Abstract

Work on foldamers, non-biological oligomers that mimic the hierarchical structure of biomacromolecules, continues to yield new architectures of ever increasing complexity. *o*-Phenylenes, a class of helical aromatic foldamers, are well-suited to this area because of their structural simplicity and the straightforward characterization of their folding in solution. However, control of structure requires, by definition, control over folding handedness. Control over *o*-phenylene twist sense is currently lacking. While chiral

induction from groups at *o*-phenylene termini has been demonstrated, it would be useful to instead direct twisting from internal positions in order to leave the ends free. Here, we explore chiral induction in a series of *o*-phenylenes with chiral imides at their centers. Conformational behavior has been studied by NMR and CD spectroscopies and DFT calculations. Chiral induction in otherwise unfunctionalized *o*-phenylenes is generally poor. However, strategic functionalization of the helix surface with trifluoromethyl or methyl groups allows it to better interact with the imide groups, greatly increasing diastereomeric excesses. The sense of chiral induction is consistent with computational models that suggest that it primarily arises from a steric effect.

1 Introduction

Foldamers, artificial oligomers that fold by analogy with biomacromolecules, have been of significant interest for decades.[1–4] Many aromatic foldamers have been developed that fold into (chiral) helical secondary structures. Unlike nature's building blocks, however, aromatic repeat units are typically not chiral. Consequently, simple aromatic foldamers will exist as (dynamic) racemates. This is an issue for any systems dependent on interactions with chiral species, including homoassembly of the foldamers themselves. Controlling helical twist sense is thus necessary to achieve full control over structure. This is typically done by attaching groups containing chirality centers at the side chains[5–10] or termini[11–17] of the oligomer, with the point chirality of these groups communicated to the helix via intramolecular interactions.

o-Phenylenes are simple class of aromatic foldamers.[18–20] An example of a perfectly folded *o*-phenylene heptamer, **oP^7**, is shown in Figure 1. The helix has three repeat units per turn, stabilizing the folded conformer through arene–arene interactions between every third repeat unit. *o*-Phenylenes are conformationally dynamic and their geometries can be studied in detail by NMR spectroscopy, making them well-suited to addressing problems in molecular folding. In recent work, we have demonstrated the coassembly of *o*-phenylenes and rod-shaped linkers into macrocycles comprising multiple foldamer subunits as simple examples of folded

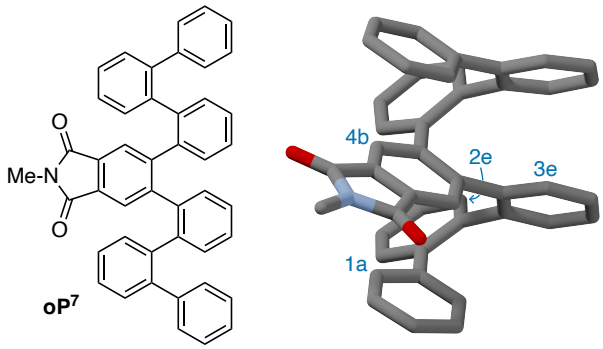

Figure 1: Model compound **oP^7** and its folded geometry (*M* helix), optimized at the PCM($CHCl_3$)/B97-D/TZV(2d,2p) level.

systems with higher-order structure.[21,22] However, there is essentially no stereocontrol in these systems: the product macrocycles comprise both twist senses of the foldamers (*M* and *P*) in statistical ratios. As a result, the products are complex racemic mixtures of multiple diastereomers. Functional systems based on the macrocycles require that the handedness of the *o*-phenylenes be controlled.

We previously reported that chiral imines[23] at the termini of *o*-phenylenes will bias their folding. The conformational behavior of these systems is complicated, however; effective interaction with the helix requires placement of the chiral groups close to the backbone, where they can then adopt multiple distinguishable orientations. Moreover, incorporating groups for chiral induction at the ends of the oligomer is not ideal for subsequent self-assembly as they block key points of attachment. It would be very useful and more modular to attach chiral directing groups at the center of the oligomer. The challenge, however, is incorporating these groups in a straightforward way while maintaining folding and interacting effectively with the surface of an *o*-phenylene helix.

Here, we report the behavior of the series of *o*-phenylene phthalimides in Chart 1.[24] Folding behavior and chiral induction in these systems was studied by a combination of NMR spectroscopy, CD spectroscopy, and computational chemistry. Good twist sense control results from not just a careful choice of the chiral group but also by modifying remote locations on the *o*-phenylene.[25]

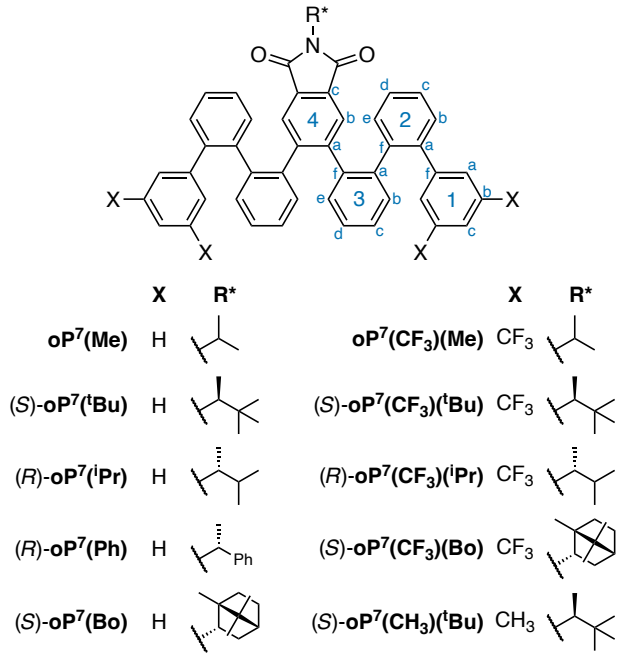

Chart 1: *o*-Phenylene heptamer phthalimides with labels used for NMR analysis.

2 Results and discussion

2.1 Design and synthesis

We targeted *o*-phenylene heptamers because they should fold with more than two full turns of the helix, ensuring slow conformational exchange on the NMR time scale. With an odd number of repeat units the chiral group can be placed in the exact center of the oligomer, simplifying analysis because most conformers should be quasi-twofold symmetric (this turned out to be more complicated than expected in some cases; see below). Scheme 1 shows the synthesis of the oligomers, which is based on standard Suzuki–Miyaura couplings using Manabe's strategy for oligophenylene synthesis.[26] Briefly, the oligomers were synthesized starting from the termini. The appropriate bromoarene was coupled with boroxarene **1** and triflated, giving trimers **2**–**4**. The triflates were then borylated (**5**–**7**) and coupled with dimethyl 4,5-diiodophthalate to give heptamers **8**–**10**. The imides were introduced by condensation of **8**–**10** with the appropriate amines.[27,28] Unfortunately, attempts to grow crystals suitable for X-ray diffraction of key compounds were unsuccessful.

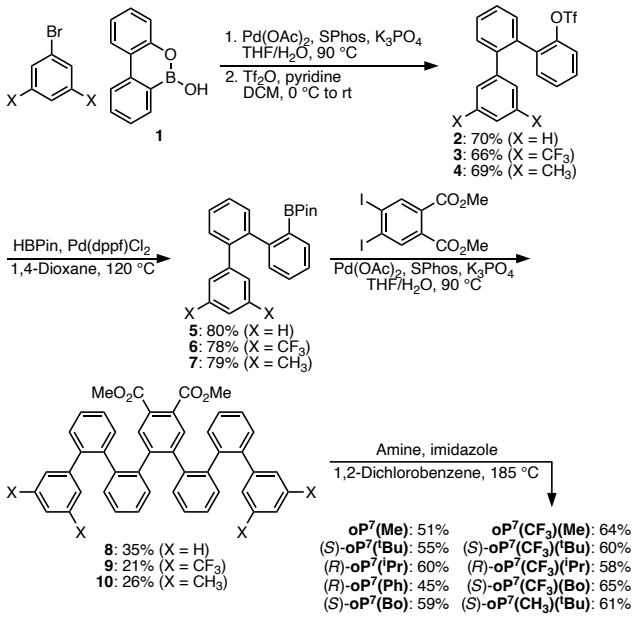

Scheme 1: Synthesis of imide-substituted *o*-phenylene heptamers.

2.2 Twist sense induction in simple *o*-phenylene phthalimides

We began by studying the series of simple, hydrogen-substituted *o*-phenylenes on the left of Chart 1. ^{1}H NMR spectra were acquired at 273 K as the signals were slightly sharper below room temperature, as is typical for *o*-phenylenes.[18] As shown in Figure 2 (top) and in the Supporting Information, the spectrum of **oP^7(Me)** is clean, with a set of major signals consistent with its structure and some smaller signals of much lower intensity. Since *o*-phenylenes of this length are in slow conformational exchange on the NMR time scale at this temperature, this indicates that the oligomer is folded into one predominant (racemic) conformation. The chemical shifts were assigned using standard 2D NMR experiments (Table S5). It is clear from comparison with the behavior of the known parent hepta(*o*-phenylene)[29] that the assignments are consistent with "perfect" folding into a compact helix analogous to that shown in Figure 1. For example, H_{4b}, H_{1a}, H_{2e}, and H_{3e}, highlighted in Figure 1, are all highly shielded compared to typical aromatic protons. In the folded state, these protons are all placed directly in the shielding zones of nearby aromatic rings. The EXSY spectrum confirms that the minor signals identified in the spectrum correspond to misfolded conformers that coexist with the major conformer (as opposed to impurities).

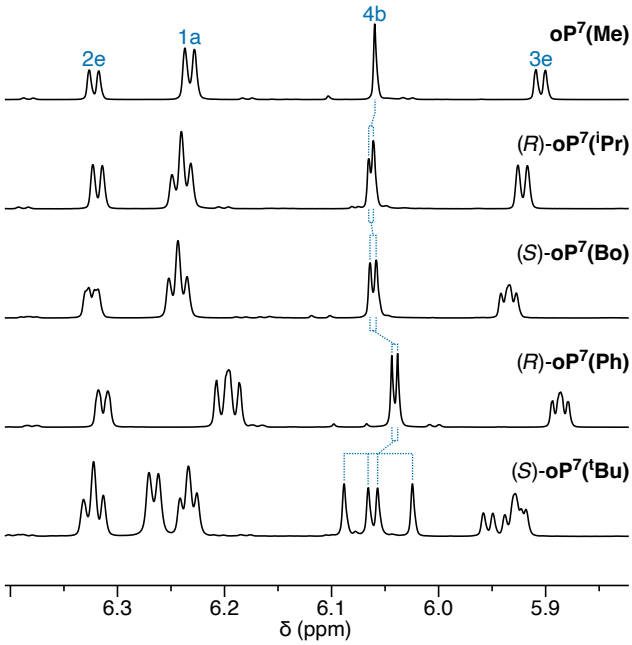

Figure 2: Partial ^{1}H NMR spectra of (*S*)-**oP^7(t Bu)**, (*R*)-**oP^7(i Pr)**, (*R*)-**oP^7(Ph)**, and (*S*)-**oP^7(Bo)** (850 MHz, $CDCl_3$, 273 K).

Integration shows that the perfectly folded conformation accounts for more than 95% of the population. This is substantially higher than for unsubstituted hepta(*o*-phenylene).[29] The electron-withdrawing imide group is expected to improve folding by strengthening the aromatic stacking interactions[30–32] that stabilize the folded state.[33] In these heptamers the imide is particularly well-located as it interacts directly with the ends of the oligomer, where misfolding tends to occur.[34]

^{1}H NMR spectra of the chiral phthalimide heptamers (*S*)-**oP^7(t Bu)**, (*R*)-**oP^7(i Pr)**, (*R*)-**oP^7(Ph)**, and (*S*)-**oP^7(Bo)** are shown in Figure 2. Despite the increased bulk of the imides, the oligomers are still predominantly well-folded (see Table S1), remaining roughly 95% well-folded on the basis of NMR integration. Signals from **oP^7(Me)** are doubled in (*R*)-**oP^7(i Pr)**, (*R*)-**oP^7(Ph)**, and (*S*)-**oP^7(Bo)** reflecting the now-inequivalent left- and right-handed helices of the *o*-phenylene. This is particularly obvious in the singlets for proton H_{4b}. Curiously, this signal is split into four for (*S*)-**oP^7(t Bu)**. We attribute this to slow rotation about the C*–N bond of the imide because of steric hindrance, which removes the effective C_2 symmetry found for the other compounds. This rationale is supported by potential energy

Compound	de (%)	Twist sense
(*S*)-**oP^7(^{t}Bu)**	4 ± 5	*M*
(*R*)-**oP^7(^{i}Pr)**	16 ± 5	*P*
(*S*)-**oP^7(Bo)**	5 ± 4	n.d.
(*R*)-**oP^7(Ph)**	6 ± 7	n.d.

Table 1: Twist sense control in (*S*)-**oP^7(^{t}Bu)**, (*R*)-**oP^7(^{i}Pr)**, (*S*)-**oP^7(Bo)**, and (*R*)-**oP^7(Ph)**.

scans for analogous maleimides (see Supporting Information); in these systems, the barrier to rotation for the *tert*-butyl-substituted compound is predicted to be 8 kcal/mol higher than that of the isopropyl-substituted compound at the PCM($CHCl_3$)/ωB97-XD/cc-pVDZ level (14 vs 6 kcal/mol).

For all compounds, the relative populations of the two diastereomeric twist senses could be obtained by deconvolution of the ^{1}H NMR spectra. Signals that were judged to give the best separation were chosen in each case, with ±10% errors assumed on each integral. The resulting diastereomeric excesses (de's) are shown in Table 1. In general, chiral induction in this series is quite low with de's essentially indistinguishable within experimental error, although that of (*R*)-**oP^7(^{i}Pr)** may be slightly higher than the others.

Chiral induction in (*S*)-**oP^7(^{t}Bu)**, (*R*)-**oP^7(^{i}Pr)**, (*R*)-**oP^7(Ph)**, and (*S*)-**oP^7(Bo)** was further studied by CD spectroscopy in chloroform at 298 K. As shown in Figure 3, each compound gives only a weak CD spectrum. For (*S*)-**oP^7(^{t}Bu)**, (*R*)-**oP^7(^{i}Pr)**, and (*S*)-**oP^7(Bo)**, the primary chromophore is the *o*-phenylene backbone itself. Indeed, the CD spectra of (*S*)-**oP^7(^{t}Bu)** and (*R*)-**oP^7(^{i}Pr)** are very similar, with characteristic Cotton effects at 250 and 280 nm. (*S*)-**oP^7(Bo)** shows a somewhat more intense band at long wavelength but is also otherwise quite similar. The CD peak intensities do not scale particularly well with the de's measured by ^{1}H NMR experiment, suggesting that the de's of (*R*)-**oP^7(^{i}Pr)** and (*S*)-**oP^7(^{t}Bu)** may be closer than suggested by the NMR measurements (note also that the two experiments were carried out a different temperatures and are not strictly comparable).

To better understand chiral induction in these systems, we optimized the geometry of model compound (*M*)-**oP^7** at the PCM($CHCl_3$)/B97-D/TZV(2d,2p) level (i.e., Figure 1) and

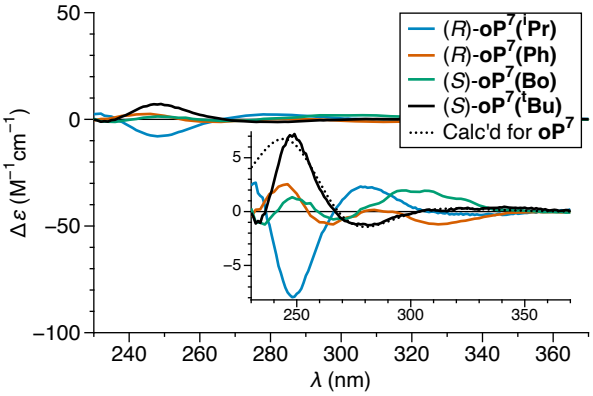

Figure 3: Experimental CD spectra of (*S*)-**oP^7(^{t}Bu)**, (*R*)-**oP^7(^{i}Pr)**, (*R*)-**oP^7(Ph)**, and (*S*)-**oP^7(Bo)** ($CHCl_3$, 298 K). The inset includes the spectrum predicted for **oP^7** in a.u. ($CHCl_3$)/CAM-B3LYP/6-311+G(2d,2p)//PCM($CHCl_3$)/B97-D/TZV(2d,2p)).

predicted its CD spectrum at the PCM($CHCl_3$)/CAM-B3LYP/6-311+G(2d,2p) level. The predicted CD spectrum of (*M*)-**oP^7** is an excellent match for the shapes of the experimental spectra of (*S*)-**oP^7(^{t}Bu)** and (*R*)-**oP^7(^{i}Pr)** (Figure 3). The calculations show that a positive Cotton effect at 250 nm is associated with an *M* absolute twist sense of the helix, indicating that (*S*)-**oP^7(^{t}Bu)** favors the *M* twist sense and (*R*)-**oP^7(^{i}Pr)** favors *P*. These are included in Table 1. The CD spectra of (*R*)-**oP^7(Ph)** and (*S*)-**oP^7(Bo)** are weak and not a good match for the DFT-predicted spectrum and so their twist senses were not assigned.

From the data, it is clear that chiral induction in this series is not very effective, with maximum de's of (16 ± 5)%. There is no obvious trend in the degree of chiral induction with the structure of the chiral group, although this may simply be lost in the significant relative uncertainties. If nothing else, it does not appear that sterics play a significant role in chiral induction in this series. That is, the *o*-phenylene helix is fairly far from the imide and presents a mostly featureless surface with no structures that would interact differently with different arrangements of groups about the chirality center.

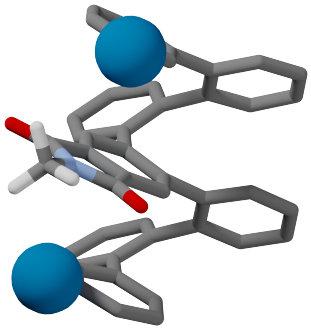

Figure 4: Substitution of the *o*-phenylene to better interact with the chiral group.

2.3 Twist sense induction in CF_3- and CH_3-substituted *o*-phenylene phthalimides

We reasoned that modifying the surface of the *o*-phenylene to better interact with the imides could increase the efficiency of chiral induction. This requires substitution of the terminal rings, which are stacked directly above and below the imide when the oligomer is folded. The positions closest to the chiral group are shown in Figure 4, corresponding to position 1b in Chart 1. We therefore designed compounds (*S*)-**oP^7(CF$_3$)(^{t}Bu)**, (*R*)-**oP^7(CF$_3$)(^{i}Pr)**, and (*S*)-**oP^7(CF$_3$)(Bo)**. Trifluoromethyl groups were chosen as they are bulky and also should maintain good folding by increasing the strength of arene–arene stacking interactions between rings 1, 4, and 7. The terminal rings were symmetrically functionalized so that their rotation would yield identical geometries, but it seems very likely that only the positions highlighted in Figure 4 should be able to interact with the chiral groups at a given time. For comparison, we also prepared methyl-substituted (*S*)-**oP^7(CH$_3$)(^{t}Bu)**.

As before, we acquired ^{1}H NMR spectra of substituted phthalimide heptamers at 273 K, shown in the Figure 5 and the Supporting Information. The spectrum of "achiral" **oP^7(CF$_3$)(Me)** is again consistent with a well-folded geometry. As shown in Table S1, overall folding remains good for the various CF_3-substituted chiral imides, with similar folding propensities to **oP^7(CF$_3$)(Me)**. Folding is generally better for the CF_3-substituted oligomers (<6% minor conformers) compared to CH_3-substituted (11% minor conformers), as expected because the electron-withdrawing CF_3 group should promote folding.[30–33] Introduction of the

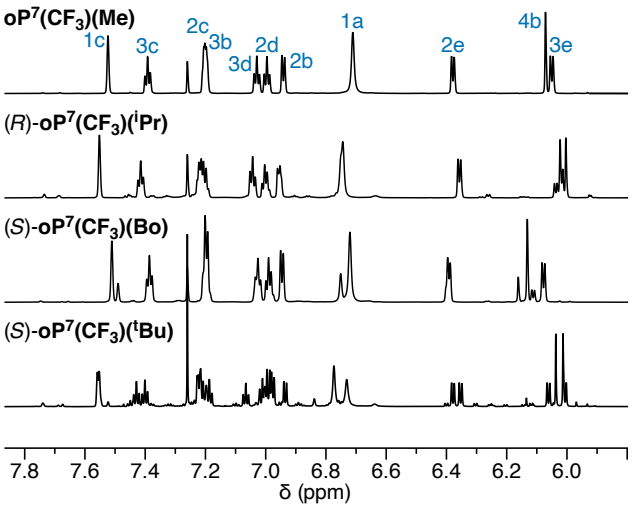

Figure 5: Partial ^{1}H NMR spectra of **oP^7(CF$_3$)(Me)**, (*R*)-**oP^7(CF$_3$)(^{i}Pr)**, (*S*)-**oP^7(CF$_3$)(Bo)**, and (*S*)-**oP^7(CF$_3$)(^{t}Bu)** (850 MHz, $CDCl_3$, 273 K).

Compound	de (%)	Twist sense
(*S*)-**oP^7(CF$_3$)(^{t}Bu)**	69 ± 10	*P*
(*R*)-**oP^7(CF$_3$)(^{i}Pr)**	36 ± 6	*M*
(*S*)-**oP^7(CF$_3$)(Bo)**	52 ± 9	*P*
(*S*)-**oP^7(CH$_3$)(^{t}Bu)**	50 ± 9	*P*

Table 2: Twist sense control in (*S*)-**oP^7(^{t}Bu)**, (*R*)-**oP^7(^{i}Pr)**, (*S*)-**oP^7(Bo)**, and (*R*)-**oP^7(Ph)**.

chiral groups again leads to signal doubling for (*R*)-**oP^7(CF$_3$)(^{i}Pr)** and (*S*)-**oP^7(CF$_3$)(Bo)** indicating distinguishable diastereomeric conformers. For the *tert*-butyl-containing (*S*)-**oP^7(CF$_3$)(^{t}Bu)** and (*S*)-**oP^7(CH$_3$)(^{t}Bu)**, we again observe signal quadrupling indicating both distinguishable diastereomers and a loss of symmetry because of slow C*–N rotation. Diastereomeric excesses were calculated by deconvolution of the ^{1}H NMR spectra and are compiled in Table 2. Overall, the substituted oligomers show marked increases in de compared to the original series.

Chiral induction in the CF_3- and CH_3-substituted phthalimide *o*-phenylenes was further studied by CD spectroscopy. As shown in Figure 6, all substituted chiral imides give significant CD bands in chloroform at 298 K, much more intense than were observed for the analogous H-substituted series. The CD peak intensities roughly correlate with the de's from the ^{1}H NMR experiments. The CD peak shapes are similar and match the spectrum calculated for

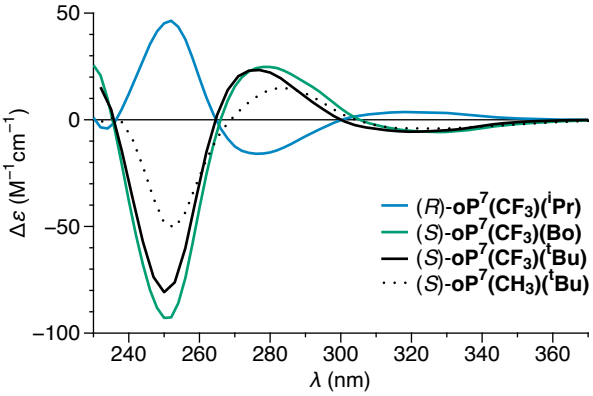

Figure 6: Experimental CD spectra of CF_3- and CH_3-substituted chiral phthalimides ($CHCl_3$, 298 K).

oP^7, with characteristic Cotton effects at 250 and 280 nm. Overall twist senses were assigned from the spectra and are included in Table 2.

Clearly, the inclusion of substituents on the *o*-phenylene gives a significant increase in the efficiency of chiral induction in this series, with a reasonably high maximum de of (69 ± 10)% for (*S*)-**oP^7(CF$_3$)(^{t}Bu)**. This corresponds to an increase in the diastereomeric ratio to 85:15 from 48:52 for the analogous (*S*)-**oP^7(^{t}Bu)**. The much more intense CD bands are also consistent with this more-effective chiral induction. Interestingly, CD spectra also show that the CF_3 and CH_3 substituents on the terminal rings invert the sense of chiral induction. That is, (*S*)-**oP^7(CF$_3$)(^{t}Bu)** gives a *P* helix (negative Cotton effect at 250 nm) whereas (*S*)-**oP^7(^{t}Bu)** gives an *M* helix (positive Cotton effect). Further, if one considers the series (*S*)-**oP^7(CF$_3$)(^{t}Bu)**, (*S*)-**oP^7(CF$_3$)(Bo)**, and (*R*)-**oP^7(CF$_3$)(^{i}Pr)**, it is clear that the degree of chiral induction increases with the increasing steric demand at the chiral center (e.g., 69% de for (*S*)-**oP^7(CF$_3$)(^{t}Bu)**, vs 36% for (*R*)-**oP^7(CF$_3$)(^{i}Pr)**). It also appears that the nature of the groups at the terminal rings affects the efficiency of chiral induction (69% de for (*S*)-**oP^7(CF$_3$)(^{t}Bu)** vs 50% for (*S*)-**oP^7(CH$_3$)(^{t}Bu)**). It seems likely that this is a simple consequence of sterics (see below), although we cannot exclude other weak interactions between the CF_3/CH_3 groups and the groups about the chirality centers.

We obtained NMR spectra of (*S*)-**oP^7(CF$_3$)(^{t}Bu)** in acetone-d_6 and benzene-d_6 to

determine whether solvent has a significant effect on the strength of chiral induction. The de's in these solvents were (72 ± 11) % and (74 ± 11)%, respectively, identical to that in chloroform within experimental error. We conclude that there is little effect, at least within the range of solvents tested, which is consistent with the generally small solvent effects found for *o*-phenylene folding.[35]

DFT calculations can be used to predict and understand the sense of chiral induction for these systems. Potential energy scans were generated for the two possible twist senses of (*S*)-**oP^7(CF$_3$)(^{t}Bu)** (see Supporting Information) and used to identify the overall conformational energy minima, which were then optimized. The results are shown in Figure 7. Different twist senses of the helix orient the chirality center and the CF_3 groups very differently with respect to each other. The calculations predict a significant difference in stability between these two conformers, 1.8 kcal/mol in favor of the (*S*,*P*) combination at the PCM($CHCl_3$)/ωB97-XD/cc-pVDZ level, which matches the experimental observation. The twist sense preference appears to be at least partly because of steric interactions; in the favored (*S*,*P*) conformer, the *tert*-butyl group is farther away from the nearest CF_3 (by 0.2 Å as measured between the nearest carbon atoms). That is, the CF_3 groups on the *P* helix are simply better positioned to fit around the groups about the *S* chirality center.

Similar calculations carried out for the analogous, unsubstituted **oP^7(^{t}Bu)** indicate that without the CF_3 groups there is a much smaller difference in stability between the two forms (see Supporting Information). The calculations do not predict an inversion of the preferred helical twist sense; the (*S*,*P*) configuration is still predicted to be favored but the difference is only 0.2 kcal/mol. While the twist sense does not match experiment, the very small difference in stability is broadly consistent with the small experimental de (4% de, equivalent to 0.04 kcal/mol). Given the very small energetic differences for the unsubstituted systems, statements about the origin of the twist sense preference are not possible.

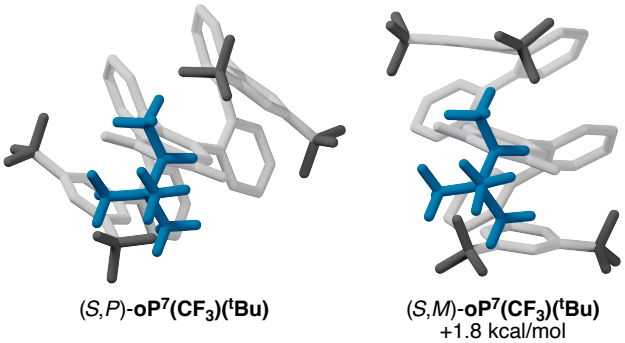

Figure 7: Optimized geometries of (*S*)-**oP^7(CF$_3$)(^{t}Bu)** with *P* and *M* twist senses (PCM($CHCl_3$)/ωB97-XD/cc-pVDZ). The models are viewed along the C*–N bond, with the chiral group (near) rendered in blue, the *o*-phenylene backbone rendered in white, and the CF_3 groups rendered in dark gray.

3 Conclusions

A set of *o*-phenylene heptamers substituted with chiral imides has been synthesized and studied by NMR and CD spectroscopies. In the absence of further substitution, chiral induction from the substituents to the *o*-phenylene is limited because of ineffective interactions between the groups about the chirality center and the helix. Strategically functionalizing the *o*-phenylene backbone with simple substituents that can interact with the imides gives both inversion of the sense of chiral induction and substantial increases in de, up to (69 ± 10)% in the best case. DFT models suggest that this is primarily a steric effect.

4 Experimental

4.1 Synthesis

4.1.1 General

Unless otherwise noted, all starting materials, reagents, and solvents were purchased from commercial sources and used without further purification. Semi-preparative gel permeation chromatography was performed using 100 Å and 500 Å polystyrene–divinylbenzene columns (300 × 21.2 mm) with toluene as the eluant at 5 mL/min. Melting points were determined

using a Thermal Analysis Q20 differential scanning calorimeter at a heating rate of 10 °C/min. NMR spectra were measured for $CDCl_3$ solutions using Bruker Avance 850, 500, or 400 MHz NMR spectrometers. Structural assignments were made with additional information from gCOSY, gHSQC, and gHMBC experiments. Boroxarene **1**,[29] dimethyl 4,5-diiodophthalate[36] and trimer **2**[29] were synthesized according to literature procedures.

4.1.2 *o*-Phenylene trimer 3

An oven-dried Schlenk vacuum tube was charged with **1** (1.50 g, 7.65 mmol), $Pd(OAc)_2$ (171.8 mg, 0.765 mmol), SPhos (628 mg, 1.53 mmol), and K_3PO_4 (4.87 g, 22.9 mmol), then evacuated and backfilled with argon (3×). To the tube, under a positive pressure of argon, was added 1,3-bis(trifluoromethyl)-5-bromobenzene (2.05 mL, 11.5 mmol), degassed THF (24 mL), and then deionized water (6 mL). The mixture was degassed by three freeze-pump-thaw cycles and filled with argon. The reaction mixture was heated at 90–95 °C (silicone oil bath) for 24 h, then cooled to room temperature and diluted with EtOAc (30 mL) and 1 M HCl(aq) (30 mL). The organic layer was separated and the aqueous layer extracted with EtOAc (3 × 20 mL). The combined organic layers were washed with brine, dried, and concentrated. Purification by flash chromatography (4:1 hexanes:EtOAc) gave the coupling product as a pale yellow liquid. The product was dissolved in CH_2Cl_2 (15 mL) and then treated with pyridine (5 equiv) and cooled to 0 °C. After 10 min, trifluoromethanesulfonic anhydride (1.5 equiv) was added dropwise. The reaction was allowed to warm to room temperature and stirred overnight. The reaction mixture was diluted with EtOAc (30 mL) and the organic layer washed with 1 M HCl(aq) (30 mL), water (30 mL), and brine (30 mL) then dried over $MgSO_4$, filtered, and concentrated. Purification by flash chromatography (9:1 hexanes:EtOAc) gave **3** as a white solid (1.815 g, 66% over two steps). m.p. 103.98 °C. ^{1}H NMR ($CDCl_3$, 400 MHz): δ 7.71 (s, 1H), 7.60–7.54 (m, 4H), 7.51–7.48 (m, 2H), 7.42–7.36 (m, 3H), 7.12–7.09 (d, 1H, J = 6.5 Hz). ^{13}C{^{1}H} NMR ($CDCl_3$, 101 MHz): δ 146.1, 142.8, 138.6, 134.23, 134.19, 132.7, 131.6, 131.2 (q, J = 34 Hz), 129.81, 128.77, 129.6, 129.5, 129.4, 128.9, 128.6, 123.4

(q, J = 274 Hz), 121.8, 118.2 (q, J = 321 Hz). $^{19}F\{^{1}H\}$ NMR ($CDCl_3$, 377 MHz): δ −63.2, −74.5. HRMS (EI-QTOF) m/z: (M^+) calcd for $C_{21}H_{11}F_9O_3S$ 514.0285; Found 514.0295.

4.1.3 o-Phenylene trimer 4

An oven-dried Schlenk vacuum tube was charged with **1** (0.50 g, 2.6 mmol), $Pd(OAc)_2$ (57.3 mg, 0.26 mmol), SPhos (125.6 mg, 0.30 mmol), and K_3PO_4 (1.60 g, 7.65 mmol), then evacuated and backfilled with argon (3×). To the tube, under a positive pressure of argon, was added 2-bromoanisole (0.63 mL, 5.1 mmol), degassed THF (8.0 mL), and then deionized water (2.0 mL). The mixture was degassed by three freeze-pump-thaw cycles and filled with argon. The reaction mixture was heated at 90–95 °C for 24 h (silicone oil bath) then cooled to room temperature and diluted with EtOAc (10 mL) and 1 M HCl(aq) (10 mL). The organic layer was separated and the aqueous layer extracted with EtOAc (3 × 10 mL). The combined organic layers were washed with water and brine, dried, and concentrated. Purification by flash chromatography (4:1 hexanes:EtOAc), gave the coupling product as a colorless liquid. The product was dissolved in CH_2Cl_2 (5 mL) and then treated with pyridine (5 equiv) and cooled to 0 °C. After 10 min, trifluoromethanesulfonic anhydride (1.5 equiv) was added dropwise. The reaction was allowed to warm to room temperature and stirred overnight. The reaction mixture was diluted with EtOAc (10 mL), and the organic layer washed with 1 M HCl(aq) (10 mL), water (10 mL), and brine (10 mL) then dried over $MgSO_4$, filtered, and concentrated. Purification by flash chromatography (9:1 hexanes:EtOAc) gave **4** as a colorless liquid (0.50 g, 69% over two steps). ^{1}H NMR ($CDCl_3$, 400 MHz): δ 7.48–7.30 (m, 7H), 7.14 (dd, 1H, J = 3.6, 2.2 Hz), 6.82 (s, 1H), 6.72 (s, 2H), 2.17 (s, 6H). $^{13}C\{^{1}H\}$ NMR ($CDCl_3$, 101 MHz): δ 146.6, 141.9, 140.6, 137.1, 135.5, 133.8, 133.0, 131.0, 130.1, 128.74, 128.72, 128.3, 127.9, 127.3, 127.0, 121.5, 118.2 (q, J = 321 Hz), 21.1. HRMS (EI-QTOF) m/z: (M^+) calcd for $C_{21}H_{17}F_3O_3S$ 406.0850; Found 406.0858.

4.1.4 *o*-Phenylene trimer 5

An oven-dried Schlenk vacuum tube was charged with **5** (0.70 g, 1.8 mmol) and $Pd(dppf)Cl_2$ (45.4 mg, 0.055 mmol), then evacuated and backfilled with argon (3×). To the tube, under a positive pressure of argon, was added HBPin (0.80 mL, 5.5 mmol), Et_3N (0.78 mL, 5.5 mmol), and degassed 1,4-dioxane (7.0 mL). The mixture was degassed by three freeze-pump-thaw cycles and filled with argon. The reaction mixture was heated at 120 °C overnight (silicone oil bath) then cooled to room temperature. The reaction was quenched with methanol and concentrated, then partitioned between water (10 mL) and CH_2Cl_2 (5 mL). The organic layer was separated and the aqueous layer extracted with CH_2Cl_2 (3 × 5 mL). The combined organic layers were dried over $MgSO_4$, filtered, and concentrated. Purification by flash chromatography (1:9 EtOAc:hexanes) gave compound **5** as a white solid (0.528 g, 80%). mp 91.42 °C. ^{1}H NMR ($CDCl_3$, 500 MHz): δ 7.68 (d, 1H, J = 7.3 Hz), 7.42–7.37 (m, 2H), 7.31 (td, 1H, J = 7.2 Hz), 7.25 (s, 1H), 7.22–7.13 (m, 7H), 6.93 (d, 1H, J = 7.3 Hz), 1.15 (s, 12H). $^{13}C\{^1H\}$ NMR ($CDCl_3$, 126 MHz): δ 147.5, 142.1, 141.7, 140.5, 134.1, 131.2, 130.3, 130.0, 129.6, 129.3, 127.5, 127.0, 126.2, 126.1, 125.6, 83.4, 24.6. HRMS (APCI-Orbitrap) m/z: ($[M + H]^+$) calcd for $C_{24}H_{26}BO_2$ 357.2026; Found 357.2022.

4.1.5 *o*-Phenylene trimer 6

An oven-dried Schlenk vacuum tube was charged with **3** (2.0 g, 3.9 mmol) and $Pd(dppf)Cl_2$ (95.3 mg, 0.12 mmol), then evacuated and backfilled with argon (3×). To the tube, under a positive pressure of argon, was added HBPin (1.69 mL, 11.7 mmol), Et_3N (1.62 mL, 11.7 mmol), and degassed 1,4-dioxane (20 mL). The mixture was degassed by three freeze-pump-thaw cycles and filled with argon. The reaction mixture was heated at 120 °C overnight (silicone oil bath) then cooled to room temperature. The reaction was quenched with methanol and concentrated, then partitioned between water (20 mL) and CH_2Cl_2 (10 mL). The organic layer was separated and the aqueous layer extracted with CH_2Cl_2 (3 × 10 mL). The combined organic layers were dried over $MgSO_4$, filtered, and concentrated. Purification by flash

chromatography (1:9 EtOAc:hexanes) gave compound **6** as a colorless liquid (1.488 g, 78%). ^{1}H NMR ($CDCl_3$, 400 MHz): δ 7.68 (s, 2H), 7.65 (d, 1H, J = 7.2 Hz), 7.60 (s, 1H), 7.45–7.37 (m, 3H), 7.29–7.22 (m, 3H), 6.99 (d, 1H, J = 7.1 Hz), 1.14 (s, 6H), 1.04 (s, 6H). ^{13}C{^{1}H} NMR ($CDCl_3$, 101 MHz): δ 146.4, 143.7, 142.8, 138.0, 134.7, 130.8, 130.5 (q, J = 33.2 Hz), 130.12, 130.10, 130.09, 130.05, 130.0, 129.9, 128.9, 127.6, 126.4, 123.3 (q, J = 272.7 Hz), 83.4, 24.5, 24.1. ^{19}F{^{1}H} NMR ($CDCl_3$, 377 MHz): δ −63.0. HRMS (EI-QTOF) m/z: (M^+) calcd for $C_{26}H_{23}BF_6O_2$ 492.1695; Found 492.1712.

4.1.6 *o*-Phenylene trimer 7

An oven-dried Schlenk vacuum tube was charged with **4** (0.50 g, 1.23 mmol) and $Pd(dppf)Cl_2$ (30.1 mg, 0.037 mmol), then evacuated and backfilled with argon (3×). To the tube, under a positive pressure of argon, was added HBPin (0.53 mL, 3.69 mmol), Et_3N (0.51 mL, 3.69 mmol), and degassed 1,4-dioxane (5 mL). The mixture was degassed by three freeze-pump-thaw cycles and filled with argon. The reaction mixture was heated at 120 °C overnight (silicone oil bath). The reaction was quenched with methanol and concentrated, then partitioned between water (10 mL) and CH_2Cl_2 (5 mL). The organic layer was separated and the aqueous layer extracted with CH_2Cl_2 (3 × 5 mL). The combined organic layers were dried over $MgSO_4$, filtered, and concentrated. Purification by flash chromatography (1:9 EtOAc:hexanes) gave compound **7** as a white solid (373 mg, 79%). mp 129.11 °C. ^{1}H NMR ($CDCl_3$, 500 MHz): δ 7.68 (d, 1H, J = 7.0 Hz), 7.41–7.19 (m, 6H), 7.03 (d, 1H, J = 7.4 Hz), 6.82 (s, 2H), 6.77 (s, 1H), 2.17 (s, 6H), 1.15 (s, 12H). ^{13}C{^{1}H} NMR ($CDCl_3$, 126 MHz): δ 147.9, 142.2, 141.4, 140.8, 136.6, 134.1, 130.9, 130.3, 129.4, 129.3, 129.0, 128.0, 127.7, 126.9, 126.0, 125.6, 83.2, 24.6, 21.2. HRMS (APCI-Orbitrap) m/z: ([M+H]$^+$) calcd for $C_{26}H_{30}BO_2$ 385.2339; Found 385.2334.

4.1.7 *o*-Phenylene heptamer 8

An oven-dried Schlenk vacuum tube was charged with dimethyl 4,5-diiodophthalate (0.30 g, 0.67 mmol), **5** (0.718 g, 2.01 mmol), $Pd(OAc)_2$ (15.1 mg, 0.067 mmol), SPhos (33.1 mg, 0.08 mmol), and K_3PO_4 (0.428 g, 2.01 mmol), then evacuated and backfilled with argon (3×). To the tube, under a positive pressure of argon, was added degassed THF (4.0 mL) and then deionized water (1.0 mL). The mixture was degassed by three freeze-pump-thaw cycles and filled with argon. The reaction mixture was heated at 85–90 °C (silicone oil bath) for 24 h, then cooled to room temperature and diluted with water (5 mL) and CH_2Cl_2 (5 mL). The organic layer was separated and the aqueous layer extracted with CH_2Cl_2 (3 × 5 mL). The combined organic layers were washed with brine, dried over $MgSO_4$, filtered, and concentrated. Purification by flash chromatography (2:8 EtOAc:hexanes) followed by gel permeation chromatography gave compound **8** as a white solid (153 mg, 35%). mp 248.01 °C. ^{1}H and ^{13}C NMR see Table S2. HRMS (APCI-Orbitrap) m/z: ($[M+H]^+$) calcd for $C_{46}H_{35}O_4$ 651.2535; Found 651.2522.

4.1.8 *o*-Phenylene heptamer 9

An oven-dried Schlenk vacuum tube was charged with dimethyl 4,5-diiodophthalate (0.50 g, 1.1 mmol), **6** (1.65 g, 3.35 mmol), $Pd(OAc)_2$ (25.2 mg, 0.112 mmol), SPhos (55.2 mg, 0.134 mmol), and K_3PO_4 (0.714 g, 3.36 mmol), then evacuated and backfilled with argon (3×). To the tube, under a positive pressure of argon, was added degassed THF (8.0 mL) and then deionized water (2.0 mL). The mixture was degassed by three freeze-pump-thaw cycles and filled with argon. The reaction mixture was heated at 85–90 °C (silicone oil bath) for 24 h, then cooled to room temperature and diluted with water (10 mL) and CH_2Cl_2 (5 mL). The organic layer was separated and the aqueous layer extracted with CH_2Cl_2 (3 × 5 mL). The combined organic layers were washed with brine, dried over $MgSO_4$, filtered, and concentrated. Purification by flash chromatography (2:8 EtOAc:hexanes) followed by gel permeation chromatography gave compound **9** as a white solid (218 mg, 21%). mp

246.71 °C. ^{1}H and ^{13}C NMR, see Table S3. HRMS (ESI-Orbitrap) m/z: ([M+H]$^{+}$) calcd for $C_{50}H_{31}F_{12}O_4$ 923.2031; Found 923.2095.

4.1.9 *o*-Phenylene heptamer 10

An oven-dried Schlenk vacuum tube was charged with dimethyl 4,5-diiodophthalate (0.25 g, 0.56 mmol), **7** (0.645 g, 1.68 mmol), $Pd(OAc)_2$ (12.6 mg, 0.056 mmol), SPhos (27.61 g, 0.067 mmol), and K_3PO_4 (0.357 g, 1.68 mmol), then evacuated and backfilled with argon (3×). To the tube, under a positive pressure of argon, was added degassed THF (4.0 mL) and then deionized water (1.0 mL). The mixture was degassed by three freeze-pump-thaw cycles and filled with argon. The reaction mixture was heated at 85–90 °C (silicone oil bath) for 24 h then cooled to room temperature and diluted with water (5 mL) and CH_2Cl_2 (5 mL). The organic layer was separated and the aqueous layer extracted with CH_2Cl_2 (3 × 5 mL). The combined organic layers were washed with brine, dried over $MgSO_4$, filtered, and concentrated. Purification by flash chromatography (2:8 EtOAc:hexanes) followed by gel permeation chromatography gave compound **10** as a white solid (103 mg, 26%). mp 187.37 °C. ^{1}H and ^{13}C NMR see Table S4. HRMS (ESI-Orbitrap) m/z: ([M+H]$^{+}$) calcd for $C_{50}H_{43}O_4$ 707.3161; Found 707.3184.

4.1.10 General procedure for phthalimide formation

An oven-dried Schlenk tube was charged with *o*-phenylene heptamer diester (1 equiv) and imidazole (30 equiv), then evacuated and backfilled with argon (3×). To the tube, under a positive pressure of argon, was added the appropriate amine (3.5 equiv) and degassed 1,2-dichlorobenzene. The mixture was degassed by three freeze-pump-thaw cycles and filled with argon. The reaction mixture was heated at 185 °C (silicone oil bath) for 24 h, then poured into methanol while hot. The resulting precipitate was collected via vacuum filtration and the precipitate washed with water. The crude product was purified by flash chromatography (1:9 EtOAc:hexanes).

4.1.11 *o*-Phenylene heptamer oP^7(Me)

Following the general procedure with **8** (0.050 g, 0.076 mmol) and isopropylamine (23 µL) gave **oP^7(Me)** as a white solid (25 mg, 51%). mp 369.08 °C. ^{1}H and ^{13}C NMR see Table S5. HRMS (APCI-Orbitrap) m/z: ([M+H]$^+$) calcd for $C_{47}H_{36}NO_2$ 646.2746; Found 646.2737.

4.1.12 *o*-Phenylene heptamer (*S*)-oP^7(^{t}Bu)

Following the general procedure with **8** (0.060 g, 0.092 mmol) and (*S*)-(+)-3,3-dimethylamine-2-butylamine (44 µL) gave (*S*)-**oP^7(^{t}Bu)** as a white solid (35 mg, 55%). mp 339.34 °C. ^{1}H and ^{13}C NMR see Table S6. HRMS (APCI-Orbitrap) m/z: ([M+H]$^+$) calcd for $C_{50}H_{42}NO_2$ 688.3216; Found 688.3211.

4.1.13 *o*-Phenylene heptamer (*R*)-oP^7(^{i}Pr)

Following the general procedure with **8** (0.065 g, 0.099 mmol) and (*R*)-(−)-2-amino-3-methyl butane (41 µL) gave (*R*)-**oP^7(^{i}Pr)** as a white solid (40 mg, 60%). mp 345.98 °C. ^{1}H and ^{13}C NMR see Table S7. HRMS (APCI-Orbitrap) m/z: ([M+H]$^+$) calcd for $C_{49}H_{40}NO_2$ 674.3059; Found 674.3052.

4.1.14 *o*-Phenylene heptamer (*R*)-oP^7(Ph)

Following the general procedure with **8** (0.095 g, 0.145 mmol) and (*R*)-(+)-1-phenylethylamine (66 µL) gave (*R*)-**oP^7(Ph)** as a white solid (46 mg, 45%). mp 289.37 °C. ^{1}H and ^{13}C NMR see Table S8. HRMS (APCI-Orbitrap) m/z: ([M+H]$^+$) calcd for $C_{52}H_{38}NO_2$ 708.2903; Found 708.2902.

4.1.15 *o*-Phenylene heptamer (*S*)-oP^7(Bo)

Following the general procedure with **8** (0.057 g, 0.087 mmol) and (*R*)-(+)-bornylamine (47 µL) gave (*S*)-**oP^7(Bo)** as a white solid (38 mg, 59%). mp 288.51 °C. ^{1}H and ^{13}C NMR see

Table S9. HRMS (APCI-Orbitrap) m/z: ([M+H]$^+$) calcd for $C_{54}H_{46}NO_2$ 740.3529; Found 740.3533.

4.1.16 *o*-Phenylene heptamer oP^7(CF$_3$)(Me)

Following the general procedure with **9** (0.078 g, 0.084 mmol), and isopropylamine (25 µL) gave **oP^7(CF$_3$)(Me)** as a white solid (50 mg, 64%). mp 294.58 °C. ^{1}H and ^{13}C NMR see Table S10. HRMS (APCI-Orbitrap) m/z: ([M+H]$^+$) calcd for $C_{51}H_{32}F_{12}NO_2$ 918.2241; Found 918.2244.

4.1.17 *o*-Phenylene heptamer (*S*)-oP^7(CF$_3$)(^{t}Bu)

Following the general procedure with **9** (0.087 g, 0.094 mmol) and (*S*)-(+)-3,3-dimethylamine 2-butylamine (45 µL) gave (*S*)-**oP^7(CF$_3$)(^{t}Bu)** as a white solid (54 mg, 60%). mp 256.46 °C. ^{1}H and ^{13}C NMR see Table S11. HRMS (APCI-Orbitrap) m/z: ([M+H]$^+$) calcd for $C_{54}H_{38}F_{12}NO_2$ 960.2711; Found 960.2715.

4.1.18 *o*-Phenylene heptamer (*R*)-oP^7(CF$_3$)(^{i}Pr)

Following the general procedure with **9** (0.076 g, 0.082 mmol) and (*R*)-(−)-2-amino-3-methyl butane (33 µL) gave (*R*)-**oP^7(CF$_3$)(^{i}Pr)** as a white solid (45 mg, 58%). mp 249.82 °C. ^{1}H and ^{13}C NMR see Table S12. HRMS (APCI-Orbitrap) m/z: ([M+H]$^+$) calcd for $C_{53}H_{36}F_{12}NO_2$ 946.2554; Found 946.2559.

4.1.19 *o*-Phenylene heptamer (*S*)-oP^7(CF$_3$)(Bo)

Following the general procedure with **9** (0.09 g, 0.097 mmol), and (*R*)-(+)-bornylamine (52 µL) gave (*R*)-**oP^7(CF$_3$)(Bo)** as a white solid (64 mg, 65%). mp 315.66 °C. ^{1}H and ^{13}C NMR see Table S13. HRMS (APCI-Orbitrap) m/z: ([M+H]$^+$) calcd for $C_{58}H_{42}F_{12}NO_2$ 1012.3024; Found 1012.3029.

4.1.20 *o*-Phenylene heptamer (*S*)-oP^7(CH_3)(^{t}Bu)

Following the general procedure with **10** (0.078 g, 0.11 mmol) and (*S*)-(+)-3,3 dimethyl-2-butylamine (53 µL) gave (*S*)-**oP^7(CH_3)(^{t}Bu)** as a white solid (50 mg, 61%). mp 244.11 °C. ^{1}H and ^{13}C NMR see Table S14. HRMS (APCI-Orbitrap) m/z: ([M+H]$^+$) calcd for $C_{54}H_{50}NO_2$ 744.3842; Found 744.3843.

4.2 UV–vis, fluorescence, and CD spectroscopy

Spectra were acquired for solutions in spectroscopy-grade chloroform. UV–vis spectroscopy was performed on a Perkin Elmer Lambda 35 UV–vis spectrometer in a 1.0 cm rectangular quartz cuvette for 10 µM solutions. Data was collected from 700 to 200 nm at 25 °C. Fluorescence spectroscopy was performed on a Perkin Elmer LS 50 fluorometer in a 1.0 cm rectangular quartz cuvette at 25 °C. Emission spectra are corrected. The absorbance at the excitation wavelength was kept below 0.1 to avoid the inner filter effect. CD spectroscopy was performed on an Aviv Model 435 Circular Dichroism Spectrometer in a rectangular 0.1 cm quartz cuvette for 300 µM solutions. Data was collected from 370 to 230 nm with an average of 15 scans per sample with 2 nm bandwidth at 25 °C. The CD spectrum for each phthalimide was obtained by subtracting the blank chloroform spectrum from the sample's raw CD spectrum.

Acknowledgements

We thank the National Science Foundation for support of this work (CHE-1904236) and the purchase of the 400 MHz NMR spectrometer (CHE-1919850).

Supporting Information

UV–vis and fluorescence spectra; NMR assignments for *o*-phenylene oligomers; computational chemistry data; NMR spectra (PDF)

Cartesian coordinates for optimized geometries (TXT)

The data underlying this study are openly available in the *Miami Scholarly Commons* at http://hdl.handle.net/2374.MIA/6835.

References

(1) Gellman, S. H. Foldamers: a manifesto. *Acc. Chem. Res.* **1998**, *31*, 173–180.

(2) Hill, D. J.; Mio, M. J.; Prince, R. B.; Hughes, T. S.; Moore, J. S. A field guide to foldamers. *Chem. Rev.* **2001**, *101*, 3893–4011.

(3) Guichard, G.; Huc, I. Synthetic foldamers. *Chem. Commun.* **2011**, *47*, 5933–5941.

(4) Le Bailly, B. A. F.; Clayden, J. Dynamic foldamer chemistry. *Chem. Commun.* **2016**, *52*, 4852–4863.

(5) Hua, Y.; Flood, A. H. Flipping the switch on chloride concentrations with a light-active foldamer. *J. Am. Chem. Soc.* **2010**, *132*, 12838–12840.

(6) Kudo, M.; Maurizot, V.; Kauffmann, B.; Tanatani, A.; Huc, I. Folding of a linear array of α-amino acids within a helical aromatic oligoamide frame. *J. Am. Chem. Soc.* **2013**, *135*, 9628–9631.

(7) Prince, R. B.; Brunsveld, L.; Meijer, E. W.; Moore, J. S. Twist sense bias induced by chiral side chains in helically folded oligomers. *Angew. Chem., Int. Ed.* **2000**, *39*, 228–230.

(8) Kudo, M.; Hanashima, T.; Muranaka, A.; Sato, H.; Uchiyama, M.; Azumaya, I.; Hirano, T.; Kagechika, H.; Tanatani, A. Identification of absolute helical structures of aromatic multilayered oligo(*m*-phenylurea)s in solution. *J. Org. Chem.* **2009**, *74*, 8154–8163.

(9) Sinkeldam, R. W.; van Houtem, M. H. C. J.; Pieterse, K.; Vekemans, J. A. J. M.; Meijer, E. W. Chiral poly(ureidophthalimide) foldamers in water. *Chem.—Eur. J.* **2006**, *12*, 6129–6137.

(10) Jang, H. B.; Choi, Y. R.; Jeong, K.-S. Matched and mismatched phenomena in the helix orientation bias induced by chiral appendages at multiple positions of indolocarbazole-pyridine hybrid foldamers. *J. Org. Chem.* **2018**, *83*, 5123–5131.

(11) Zheng, L.; Zhan, Y.; Yu, C.; Huang, F.; Wang, Y.; Jiang, H. Controlling helix sense at N- and C-termini in quinoline oligoamide foldamers by β-pinene-derived pyridyl moieties. *Org. Lett.* **2017**, *19*, 1482–1485.

(12) Liu, Z.; Hu, X.; Abramyan, A. M.; Mészáros, Á.; Csékei, M.; Kotschy, A.; Huc, I.; Pophristic, V. Computational prediction and rationalization, and experimental validation of handedness induction in helical aromatic oligoamide foldamers. *Chem.—Eur. J.* **2017**, *23*, 3605–3615.

(13) Kayamori, F.; Abe, H.; Inouye, M. Stabilization of chiral helices for saccharide-linked ethynylpyridine oligomers possessing a conformationally well-defined linkage. *Eur. J. Org. Chem.* **2013**, *2013*, 1677–1682.

(14) Hu, H.-Y.; Xiang, J.-F.; Yang, Y.; Chen, C.-F. Chiral induction in phenanthroline-derived oligoamide foldamers: an acid- and base-controllable switch in helical molecular strands. *Org. Lett.* **2008**, *10*, 1275–1278.

(15) Naidu, V. R.; Kim, M. C.; Suk, J.-m.; Kim, H.-J.; Lee, M.; Sim, E.; Jeong, K.-S. Biased helical folding of chiral oligoindole foldamers. *Org. Lett.* **2008**, *10*, 5373–5376.

(16) Mazzier, D.; Crisma, M.; De Poli, M.; Marafon, G.; Peggion, C.; Clayden, J.; Moretto, A. Helical foldamers incorporating photoswitchable residues for light-mediated modulation of conformational preference. *J. Am. Chem. Soc.* **2016**, *138*, 8007–8018.

(17) Kendhale, A. M.; Poniman, L.; Dong, Z.; Laxmi-Reddy, K.; Kauffmann, B.; Ferrand, Y.; Huc, I. Absolute control of helical handedness in quinoline oligoamides. *J. Org. Chem.* **2010**, *76*, 195–200.

(18) Hartley, C. S. Folding of *ortho*-phenylenes. *Acc. Chem. Res.* **2016**, *49*, 646–654.

(19) Ohta, E.; Sato, H.; Ando, S.; Kosaka, A.; Fukushima, T.; Hashizume, D.; Yamasaki, M.; Hasegawa, K.; Muraoka, A.; Ushiyama, H.; Yamashita, K.; Aida, T. Redox-responsive molecular helices with highly condensed π-clouds. *Nat. Chem.* **2011**, *3*, 68–73.

(20) Blake, A. J.; Cooke, P. A.; Doyle, K. J.; Gair, S.; Simpkins, N. S. Poly-*ortho*phenylenes: synthesis by Suzuki coupling and solid state helical structures. *Tetrahedron Lett.* **1998**, *39*, 9093–9096.

(21) Kinney, Z. J.; Kirinda, V. C.; Hartley, C. S. Macrocycles of higher *ortho*-phenylenes: assembly and folding. *Chem. Sci.* **2019**, *10*, 9057–9068.

(22) Kirinda, V. C.; Hartley, C. S. Folding-controlled assembly of *ortho*-phenylene-based macrocycles. *Chem. Sci.* **2021**, *12*, 6992–7002.

(23) Vemuri, G. N.; Pandian, R. R.; Spinello, B. J.; Stopler, E. B.; Kinney, Z. J.; Hartley, C. S. Twist sense control in terminally functionalized *ortho*-phenylenes. *Chem. Sci.* **2018**, *9*, 8260–8270.

(24) The bornyl-substituted phthalimides are made from (*R*)-bornylamine. We classify them as *S*, referring to the chirality center attached directly to the N, for consistency with the other oligomers.

(25) An initial version of this work was deposited in *ChemRxiv* on Jul. 27, 2022, Reference DOI: 10.26434/chemrxiv-2022-9r7nl.

(26) Ishikawa, S; Manabe, K Repetitive two-step method for oligoarene synthesis through rapid cross-coupling of hydroxyphenylboronic acids and anhydrides. *Chem. Lett.* **2006**, *35*, 164–165.

(27) Feng, C.; Ding, Y.-H.; Han, X.-D.; Yu, W.-H.; Xiang, S.-K.; Wang, B.-Q.; Hu, P.; Li, L.-C.; Chen, X.-Z.; Zhao, K.-Q. Triphenylene 2, 3-dicarboxylic imides as luminescent liquid crystals: Mesomorphism, optical and electronic properties. *Dyes Pigm.* **2017**, *139*, 87–96.

(28) Psutka, K. M.; LeDrew, J.; Taing, H.; Eichhorn, S. H.; Maly, K. E. Synthesis and self-assembly of liquid crystalline triphenylenedicarboxythioimides. *J. Org. Chem.* **2019**, *84*, 10796–10804.

(29) Mathew, S. M.; Hartley, C. S. Parent *o*-phenylene oligomers: synthesis, conformational behavior, and characterization. *Macromolecules* **2011**, *44*, 8425–8432.

(30) Wheeler, S. E.; Bloom, J. W. G. Toward a more complete understanding of noncovalent interactions involving aromatic rings. *J. Phys. Chem. A* **2014**, *118*, 6133–6147.

(31) Hwang, J.; Li, P.; Carroll, W. R.; Smith, M. D.; Pellechia, P. J.; Shimizu, K. D. Additivity of substituent effects in aromatic stacking interactions. *J. Am. Chem. Soc.* **2014**, *136*, 14060–14067.

(32) Hunter, C.; Lawson, K.; Perkins, J; Urch, C. Aromatic interactions. *J. Chem. Soc., Perkin Trans. 2* **2001**, 651–669.

(33) Mathew, S.; Crandall, L. A.; Ziegler, C. J.; Hartley, C. S. Enhanced helical folding of *ortho*-phenylenes through the control of aromatic stacking interactions. *J. Am. Chem. Soc.* **2014**, *136*, 16666–16675.

(34) Hartley, C. S.; He, J. Conformational analysis of *o*-phenylenes: helical oligomers with frayed ends. *J. Org. Chem.* **2010**, *75*, 8627–8636.

(35) Vemuri, G. N.; Chu, M.; Dong, H.; Spinello, B. J.; Hartley, C. S. Solvent effects on the folding of *o*-phenylene oligomers. *Org. Biomol. Chem.* **2017**, *15*, 845–851.

(36) Hisaki, I.; Sakamoto, Y.; Shigemitsu, H.; Tohnai, N.; Miyata, M. Conformational polymorphism of octadehydrodibenzo[12]annulene with dimethyl phthalate moieties. *Cryst. Growth Des.* **2008**, *9*, 414–420.